Hydrostatic Fluid-structure Characteristic Analysis of Hydraulically Damped Rubber Mount

LirngWang, Zhenhua LU, and Ichiro Hagiwara.

Abstract—**A modeling approach of HDM based mixed finite element formulation of hydrostatic fluid-structure interaction is introduced. Fluid transfer analysis of mass flow rate versus pressure difference through fluid track between two chambers is carried out. The finite element models of upper and lower chambers are bridged through the fluid transfer analysis. Static working process of a typical HDM with fixed decoupler is simulated. The agreeable comparison of static elasticity with experimental result verifies the effectiveness and practicability of the proposed approach.**

Index Terms—**Elastic characteristic, Hydraulically damped rubber mount, Fluid-structure interaction, Engine mount, Volumetric characteristic..**

I. Introduction

Vehicle powertrain mounting system (PMS) plays a important role in automotive NVH (Noise, Vibration and Harshness) control. Hydraulically damped rubber mount (HDM) is a kind of effective isolator to support to powertrain and to attenuate vibrations transmitting between powertrain and body/chassis and to reduce the interior noise of vehicle compartment.

In HDM, fluid transfers between the two chambers through fluid track. Moreover, the fluid-structure interactions (FSI) in chambers between fluid and rubber parts like rubber spring, diaphragm and decoupler membrane have great influence to performance of HDM. The fluid transfer characteristic and FSI in HDM results in distinguish performance of HDM comparing with that of rubber mount without fluid chambers. In the early study stage of HDM, fluid and structure are considered separated by conventional lumped-parametric model. In 1990s, with the development of finite elemen (FE) analysis, FE analysis is introduced into characteristic research of HDM, Karlheinz presented FE modelling theory of rubber mountings with hydraulic damping [1], and Gotz developed a computer-aided concept for analysis and design of HDM with FE method to obtain stiffness and volumetric elasticity [2]. Shibayama. et al predicted fluid track resistance by using CFD (Computational fluid dynamic) code [3]. With development of computational fluid dynamics and FE approach in fluid computation, modeling and simulation approaches of HDM has made great progress. A kind of FE simulation approach on the base of an ALE-based strong coupling fluid-structure interaction (FSI) FE formulation is investigated by Wang [4]. However, the problem in fully coupling FE analysis in FSI of HDM is the heavy modeling and computational workload.

This paper presents a convenient hydrostatic fluid-structure characteristic analysis approach of HDM, which integrates fluid transfer performance analysis in fluid track and the FSI FE models of fluid chambers with consideration of fluid-structure interaction between rubber components and fluid in chambers. This hydrostatic FSI analysis of HDM is suitable to carry out static performance of HDM considering fluid flow transfer between chambers and fluid-rubber interaction in chambers, to conduct volumetric capacity design of fluid chamber, and to evaluate carrying capacity and static elasticity. Such integration of hydrostatic FSI modeling approach with lumped-parametric modeling of fluid track can relieve of the heavy computational cost in the FE analysis with full element coupling model of FSI in HDM.

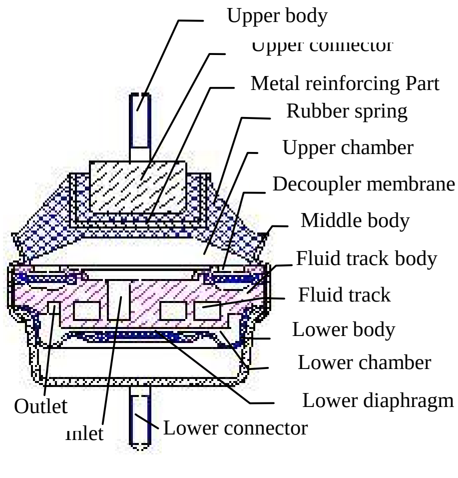

Fig. 1. HDM Structure

Manuscript received March 31, 2009.

Wang lirong is professor in Shenzhen institute of advanced technology, Chinese academy of sciences and an adjunct associate professor in Tokyo Institute of Technology, 2-12-1, O-okayama, Meguro-ku, Tokyo, 152-8552, Japan (phone: 81-80-6664-0068; fax: 81-3-5734-2893; e-mail: lrwang@ mails.tsinghua.edu.cn).

LU zhenhua was with Tsinghua University, Beijing, 100084, Beijing China. (e-mail: lvzh@tsinghua.edu.cn).

Hagiwara ichiro is with Tokyo Institute of Technology, 2-12-1, O-okayama, Meguro-ku, Tokyo, 152-8552, Japan (e-mail: hagiwar@mech.titech.ac.jp).

ISBN:978-988-18210-1-0

II. FLUID TRANSFER PERFORMANCE ANALYSIS

A. HDM Structure

A typical HDM used in a vehicle powertrain system is chosen for this study. Fig. 1 shows the structure of the HDM, which is mainly composed of a rubber spring, two fluid chambers, a fluid track and a decoupler membrane. Among them, the rubber spring possessing high elasticity serves as main support of powertrain load and as a piston to pump fluid to flow between upper and lower chambers through fluid track. The main physical property of rubber spring is characterized by its elastic stiffness and damping. Fluid track plays a role as tuned isolation damper. Fluid flow between the two chambers results in the change of fluid volume of the two chambers. For interaction problems in HDM, fluid forces applied onto rubber components deform rubber components, and deformations of rubber components result in the change of fluid domain. Decoupler membrane helps to increase volumetric elasticity of upper chamber to achieve good isolation when there is less fluid flowing between chambers.

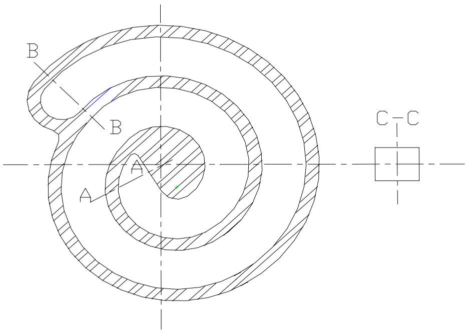

Fig. 2. Mechanical model of fluid track

B. Fluid transfer performance in fluid track

The fluid track plays an important role in controlling fluid flowing between upper and lower chambers, which further influences fluid fields in chambers and deformations of rubber parts, and finally has effect on HDM performance. Fluid transfer performance through fluid track is studied based on fluid mechanics model shown in Fig. 2, which is set up according to the following assumptions:

- Fluid is incompressible.
- Influence of gravity is neglected.
- Properties are uniform at sections A-A and B-B.
- Relative velocity of fluid along the track is constant.
- Cross sections between A-A and B-B along the track have the same shape.

The fluid mathematical model established according to Bernoulli equation [5] can be expressed in mass flow rate format as

$$\dot{Q}_m + \frac{1}{2\rho AL}\left(\frac{f_l L}{D_h} + \xi\right) Q_m^{\ 2} sign(Q_m) = \frac{A}{L}\Delta p \qquad (1)$$

where $\Delta p = p_1 - p_2$ is the pressure difference between inlet and outlet of fluid track. p_1 and p_2 are average pressure on the section A-A and section B-B, respectively, as shown in Fig.2. Q_m is mass flow rate, and $Q_m = \rho A v_x$, here v_x is flow velocity along fluid stream line, A cross-section area of fluid track, ρ fluid density. *sign* is sign function.

Table 1 The relationship between fluid state and major loss coefficient

Fluid state	R_e	Major loss coefficient f_l
Laminar flow	$R_e \le 2000$	$f_l = \frac{64}{R_e}$
Transition region	$2000 < R_e \le 4000$	$f_l = \frac{(f_{l1} - f_{l2})}{2000} R_e + 2 f_{l2} - f_{l1}$ $f_{l2} = 64 / R_1$，$f_{l1} = \left[-2\log_{10}\left(\frac{\delta}{3.7} + \frac{2.51}{4000\sqrt{f_{l1}}}\right)\right]$
Turbulence flow (1)	$4000 < R_e \le 5000/\delta$	$\frac{1}{\sqrt{f_l}} = -2\log_{10}\left(\frac{\delta}{3.7} + \frac{2.51}{R_e\sqrt{f_l}}\right)$
Turbulence flow (2)	$5000/\delta < R_e$	f_l=constant

Notice: $R_e = \frac{v_x D_h}{\mu}$ is Reynold number, where μ is kinematic viscosity, $D_h = \frac{4A}{L_h}$ the hydraulic radius of cross section of fluid track, L_n the wet periphery, $\delta = \frac{K_s}{D}$ the relative roughness, K_s the equivalent roughness determined by pipe material.

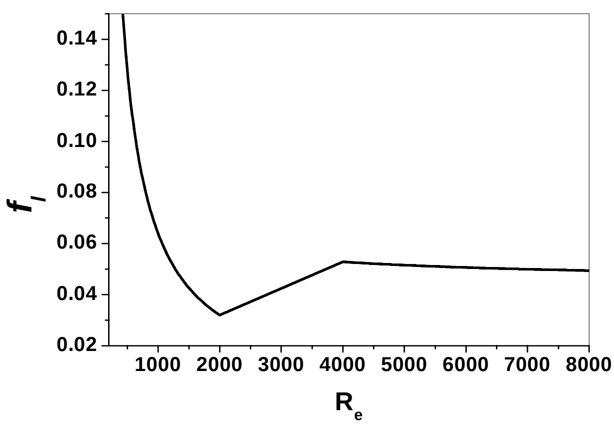

Fig. 3. Major loss coefficient versus Reynold number

Fluid resistance of R_f, $R_f = \frac{1}{2}(\frac{f_l L}{D_h} + \xi)v_x^2$, includes major loss and minor loss in fluid track. Major loss is expressed as $\frac{f_l L}{2D_h}v_x^2$, where L is length of fluid track, and D_h is hydraulic radius of cross section of fluid track, and major loss coefficient of f_l is dynamically estimated according to analytical formulas listed in Table 1. Fig. 3 demonstrates the relationship between f_l and Reynold number of R_e, which is obtained from the formulas in Table 1, and Reynold number can be evaluated by status of fluid flow according to formulation in Table 1. Minor loss is represented as $\frac{1}{2}\xi v_x^2$, where minor loss coefficient of ξ includes contraction loss coefficient of inlet $\xi_{11} = \frac{1}{2}(1 - \frac{A_{out}}{A_{in}})$, expansion loss coefficient of outlet $\xi_{12} = \frac{1}{2}(\frac{A_{out}}{A_{in}} - 1)$, and track bend loss coefficient determined by curvature radius and diameter of fluid track according to the empirical formulas [6], here A_{in} and A_{out} are cross area of inlet and outlet respectively.

Fluid transfer performance through fluid track can be obtained by numerical calculation of Equ. (1) using Runge-Kutta method in Matlab [7]. Figure 4 (a) shows the time response characteristic of mass flow rate Q_m under stable pressure difference Δp, which demonstrates that Q_m quickly approaches constant under a certain fluid pressure difference, and fluid flow approaches into stable state. Figure 4 (b) illustrates the nonlinear relationship between the stable Q_m and the corresponding Δp. This relationship between Q_m and Δp will be used to make a user-defined table of mass flow rate versus pressure difference for fluid link element, and to bridge the following hydrostatic FE models of upper and lower chambers.

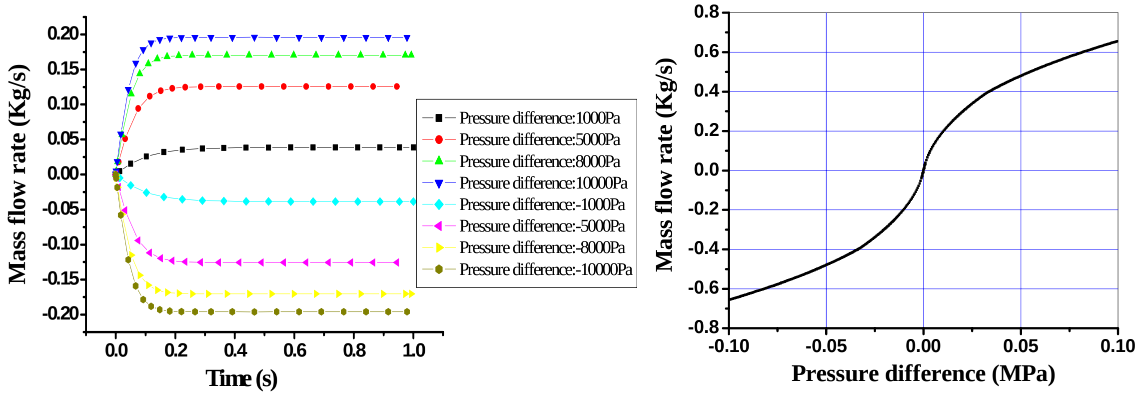

(a) $Q_m \sim t$ (b) $Q_m \sim \Delta p$

Fig. 4. Fluid transfer performance through fluid track

III. Hydrostatic Fluid-Structure Interaction Finite Element Modeling of HDM

To investigate finite element modeling is developed by using PATRAN 9.0 (1998). The numerical FE analysis is carried out by using ABAQUS/Standard Version 5.8 [8] on a supercomputer SGI Origin 2000.

As shown in Fig. 5, a quarter-symmetric model of HDM is built up based on the actual quarter-symmetry geometry. C3D8RH element (8-node linear brick, reduced integration with hourglass control, hybrid element with constant

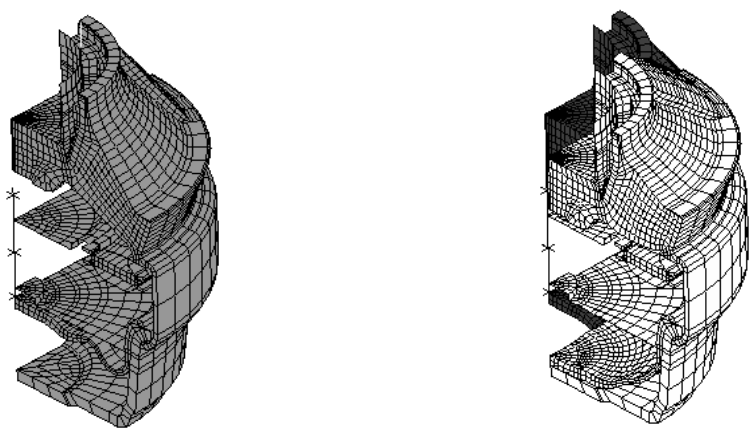

(a) FE model (b) Deformation under preload

Black line indicates undeformed configuration, White line indicates deformed configuration.

Fig. 5. Quarter-symmetric model of HDM

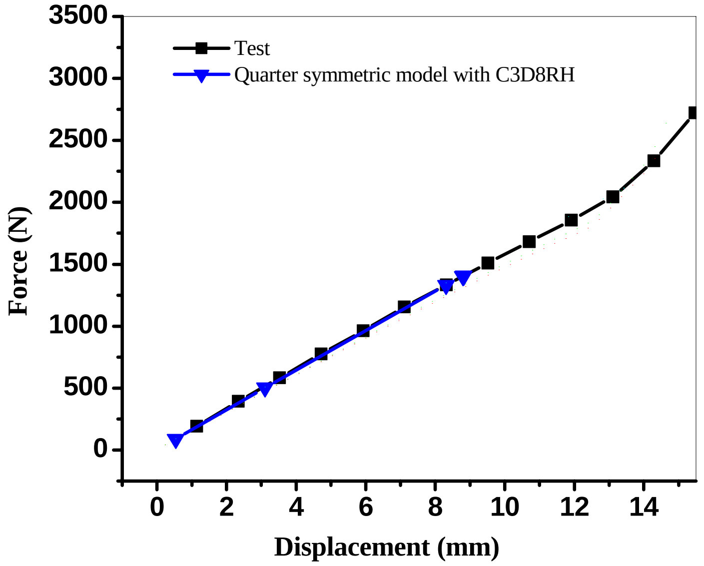

Fig. 6. Comparisons of predicted and experimental elastic characteristics of HDM

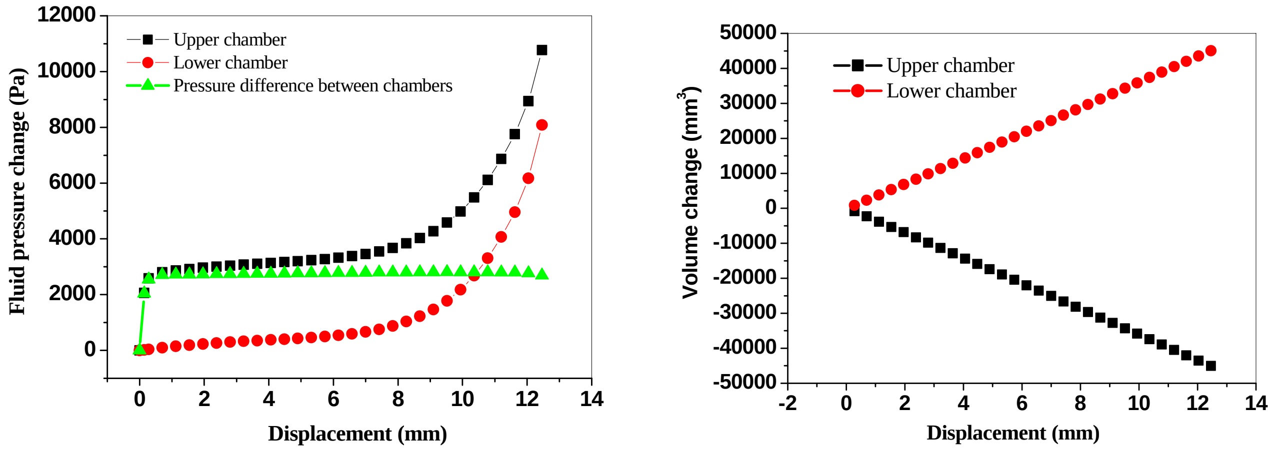

(a) Chamber fluid pressure change (b) Chamber volume change

Fig. 7. Predicted chamber fluid pressure and volume change of axisymmetric HDM model.

pressure) and C3D8H element (8-node linear brick, hybrid element with constant pressure) are used respectively to mesh the rubber parts. C3D8 element (8-node linear brick) is used to mesh middle body, metal reinforcing part in rubber spring and lower body, respectively. To avoid unnecessary computations, the upper body and fluid track body are defined as rigid bodies. Vertical loading displacement is given at the reference node of rigid upper body. The bottom surface of lower body is fixed.

F3D4 element (4-node linear hydrostatic fluid element) is chosen to model upper and lower chambers. All fluid elements on the fluid-structure interfaces, two cavity reference nodes and slave-master contact surfaces in chambers are defined in the similar way as those in the previous axisymmetric model. The relationship between Q_m and Δp in Fig. 4 (b) is used to define a fluid link element to link the two reference nodes. This quarter-symmetric model has 7821 elements, 14884 nodes and 30140 DOFs.

IV. Static Characteristic Analysis

A. Static elastic characteristic simulation

The predicted static elastic characteristics under loading of vertical displacement of the HDM is shown in Figure 6. The static characteristic shows behaves linearly before deformation reaches 12.6mm and then shows hard elasticity beyond this point, since the inner part of the rubber component is in contact with fluid track body. The normal working condition of HDM before its inner contact occurs is essential to the performance evaluation and design of HDM. Thus, elastic characteristic simulation of HDM focuses mainly on its normal working conditions. The comparison between predicted and experimental results of static elastic characteristics approves the effective of the presented modeling analysis of HDM.

B. Chamber volumetric capacity analysis

The chamber volumetric capacity analysis is one of the important design contents in HDM development to ensure suitable fluid capacity and volumetric elasticity in each

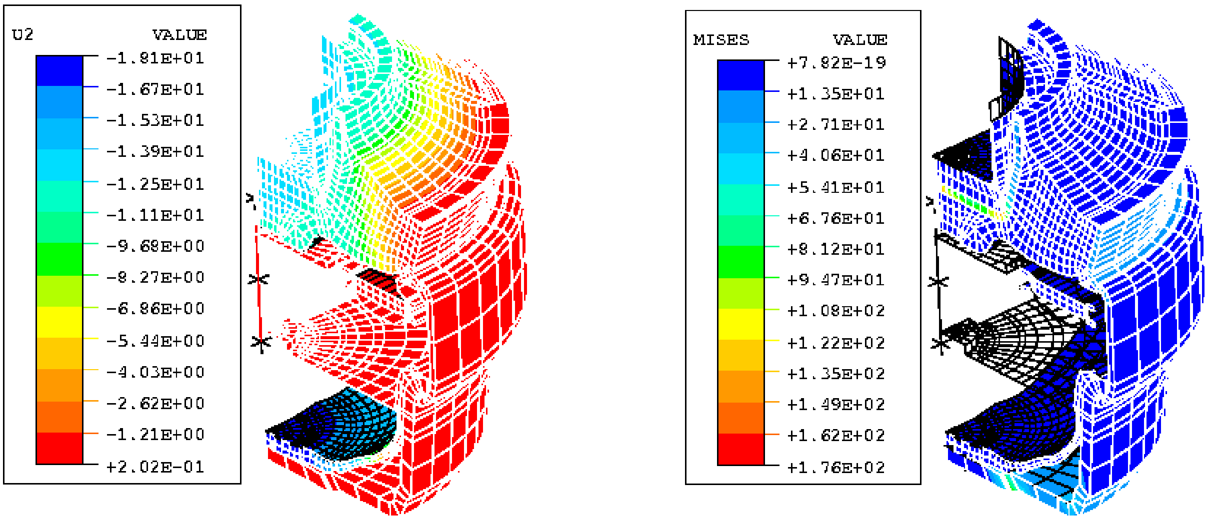

(a) Vertical displacement (mm) contours (b) von Mises stress (MPa) contours

Fig. 8. FE analysis result of HDM of quarter-symmetric model under vertical loading of 2443N

chamber and fluid transmission among chambers. The FE simulation of static working process can clarify the detailed working status of chambers such as volume change of chambers, fluid pressure change, and deformation of chambers. Fig. 7 shows the simulation results of fluid pressure and volume change of chambers of HDM. In Fig.7 (a), before the vertical displacement of 6mm is reached, the lower diaphragm keeps in a natural spread state without interior tensile force, and the fluid pressure in each chamber keeps low state. After vertical displacement of HDM reaches 6mm, the lower diaphragm is tensed, and the fluid pressure in both chambers begin to increase at the same rate. The fluid pressure difference between two chambers keeps 2740Pa, which is not met with the actual working status of HDM. The reason is that the fluid mass transfer of hydrostatic fluid-structure interaction FE method of ABAQUS considers only mass conservation but not the fluid pressure boundary condition. Such error is only 2.6% of the fluid pressure of upper chamber, which is in the permitted engineering error range. Fig. 7 (b) shows that the volume reduction of upper chamber is equal to the volume increase of lower chamber, which is agreeable to the actual working condition of HDM. Both the fluid pressure and volume change results demonstrate the effectiveness of the elasticity simulation process.

C. *Strain and stress analysis*

Fig. 8 (a) shows the vertical displacement contour of HDM. When the rubber spring just contacts with fluid track body, almost all the fluid in the upper chamber flow into lower chamber. Fig. 8 (b) shows the von Mises stress contour of HDM. The deformation of decoupler membrane under static loading is small, and its stress is also very small. Fig. 8 (b) also demonstrates the maximum von Mises stress is located on the metal reinforcing. Thus, the metal reinforcing part is the main loading support of HDM. Figure 9 illustrates the von Mises stress (MPa) contours of metal reinforcing, and its corner part is the maximum stress area. Even though the yield stress of metal is much larger than that of rubber material, the shape of metal reinforcing part directly influences deformation of rubber spring. Rubber spring is the main deformation part of HDM, and its deformation directly influences volume change of upper chamber. Fig. 10 (a) shows the detail vertical displacement of lower diaphragm, which demonstrates that the maximum displacement is in the center part of lower chamber, and displacement decreases in the radial direction. During fluid flowing into lower chamber, lower diaphragm spreads with little tensile force, as shown in Fig. 10 (b), which results in the low fluid pressure increment in lower chamber and guarantees smooth fluid flowing from upper chamber to lower chamber. After all the fluid in upper chamber has flowed into lower chamber, the spread lower diaphragm is just to contact with the inner surface of lower body, which guarantees low diaphragm not to frequently contact with lower body during its frequent spread. Such chamber volumetric design and low diaphragm shape design are important to realize ideal fluid flowing status between two chambers. This proposed static elasticity simulation method helps to conveniently perform structural design and volumetric capacity design of HDM.

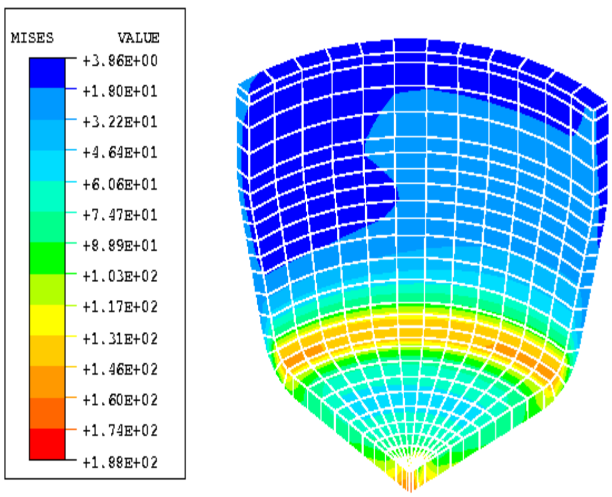

Fig. 9. von Mises stress (MPa) contours of metal reinforcing under vertical loading of 2443N

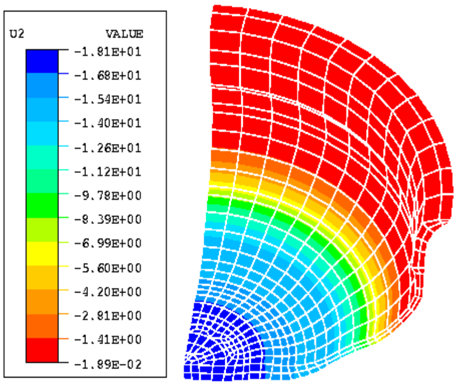

(a) Vertical displacement (mm) contours

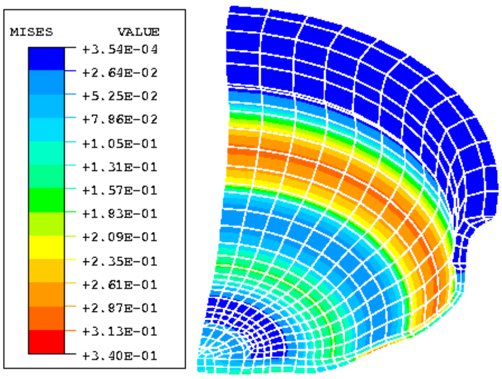

(b) von Mises stress (MPa) contours

Fig. 10. FE analysis result of quarter-symmetric model of lower diaphragm under vertical loading of 2443N

V. Conclusion

An integrated modeling technique with hydrostatic FE method of FSI and lumped-parameter based fluid transfer performance analysis through fluid track is studied to investigate the prediction of static performance of HDM. Static characteristic of a typical HDM with fixed decoupler is predicted, which is verified by comparison with experimental results. Volumetric and structural design of chambers and structural designs of low diaphragm and decoupler membrane and metal reinforcing part can be conveniently carried out. This elementary characteristic simulation method of HDM, as one optional modeling and simulation method, can help automotive engineers to carry out computer aided system technology in design and development of HDM and PMS.

Acknowledgment

The authors would also like to thank Wuxi CSI Vibration Isolators Co., Ltd, China for its assistance in testing HDM.

References

[1] K. Holzemer, “ Theorie der gummilager mit hydraulischer dampfung, ”ATZ, 87, , 1985, pp. 545-551.
[2] K. Gotz, G. Theodor and G. Dietmar, “Conputerunterstutzte Auslegung von Hydraulisch Gedampften Gummilagern, ” ATZ, 94, 1992, pp. 462-472.
[3] T. Shibayama, Y. Takashima, T. Horioka, “Theoretical investigation of the dynamic characteristic of hydraulic mount, ” JSA E, 1998, 9833278.
[4] L.R.Wang, “Study of theory and methods for simulation of nonlinear characteristics of hydraulically damped rubber mount, ” PhD Thesis, Department of Automotive Engineering, Tsinghua University, Beijing, P. R. China 2002.
[5] R.W. Fox, A.T. Mcdonald, “Introduction to Fluid Mechanics (Third Edition), ”John Wiley & Sons, New York1985.
[6] Y.Z. Li, M.S.Fan, “Fluid Mechanics, ” High Education Press, Beijing1998.
[7] Matlab 7.0 Manual, The MathWorks.
[8] ABAQUS Theory’s Manual, H. K. S. Inc., 1998.